

# Fragment-Based Design of Selective Nanomolar Ligands of the CREBBP Bromodomain

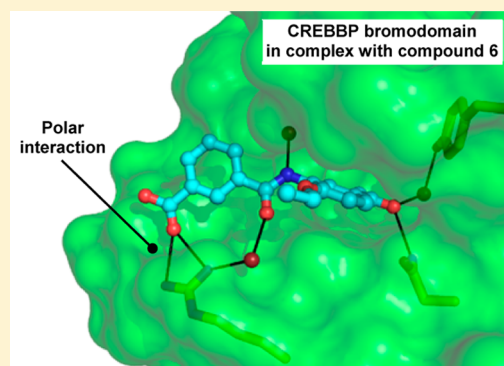
Andrea Unzue,<sup>†</sup> Min Xu,<sup>‡</sup> Jing Dong,<sup>‡</sup> Lars Wiedmer,<sup>‡</sup> Dimitrios Spiliotopoulos,<sup>‡</sup> Amedeo Caflisch,<sup>\*,‡</sup> and Cristina Nevado<sup>\*,†</sup>

<sup>†</sup>Department of Chemistry, University of Zürich, Winterthurerstrasse 190, CH-8057, Zürich, Switzerland

<sup>‡</sup>Department of Biochemistry, University of Zürich, Winterthurerstrasse 190, CH-8057, Zürich, Switzerland

## Supporting Information

**ABSTRACT:** Novel ligands of the CREBBP bromodomain were identified by fragment-based docking. The in silico discovered hits have been optimized by chemical synthesis into selective nanomolar compounds, thereby preserving the ligand efficiency. The selectivity for the CREBBP bromodomain over other human bromodomain subfamilies has been achieved by a benzoate moiety which was predicted by docking to be involved in favorable electrostatic interactions with the Arg1173 side chain, a prediction that could be verified a posteriori by the high-resolution crystal structure of the CREBBP bromodomain in complex with ligand **6** and also by MD simulations (see Xu, M.; Unzue, A.; Dong, J.; Spiliotopoulos, D.; Nevado, C.; Caflisch, A. Discovery of CREBBP bromodomain inhibitors by high-throughput docking and hit optimization guided by molecular dynamics. *J. Med. Chem.* **2015**, DOI: 10.1021/acs.jmedchem.5b00171).



## ■ INTRODUCTION

The quest for bromodomain inhibitors as potential therapeutic tools has bloomed in recent years based on the growing understanding of epigenetic processes. Post-transcriptional modifications of histone tails constitute a highly sophisticated mechanism for gene expression control,<sup>1,2</sup> in which bromodomain proteins function as readers of the so-called histone code.<sup>3–10</sup> Given the direct connection between the regulation of gene expression and physiological and pathological processes, molecules interfering with bromodomains have recently emerged as chemical probes and/or clinical tools to regulate cancer, inflammation, and other diseases. Of the 61 human bromodomains known, the BET (bromo and extraterminal) family of bromodomains seems the most druggable,<sup>4,10</sup> as several potent ligands have been reported, in particular for BRD4(1) (the first bromodomain of the BRD4 protein).<sup>11,12</sup> These bromodomains have been directly connected to inflammation, aggressive types of squamous cell carcinomas and hematological malignancies such as acute myeloid leukemia.<sup>3,6,12–15</sup> The identification of potent and selective inhibitors would be extremely useful for other bromodomains, whose direct connection to specific diseases has not yet been established in many cases. The single bromodomain in the CREB binding protein (CREBBP) is a representative example, as few small molecule ligands of this bromodomain have been reported, and high selectivity proved to be difficult to achieve.<sup>16–19</sup> In 2014, Rooney et al. reported the first nanomolar potent CREBBP inhibitors based on dihydroquinoxalinone scaffolds.<sup>20</sup> Absolute stereocontrol was required to attain the desired potency, and still only moderate

selectivity against BRD4(1), the most promiscuous bromodomain, was found. Last year, Hay et al. reported a medicinal chemistry optimization campaign for selective CREBBP bromodomain inhibitors starting from a nonselective 3,5-dimethylisoxazole ligand.<sup>21</sup>

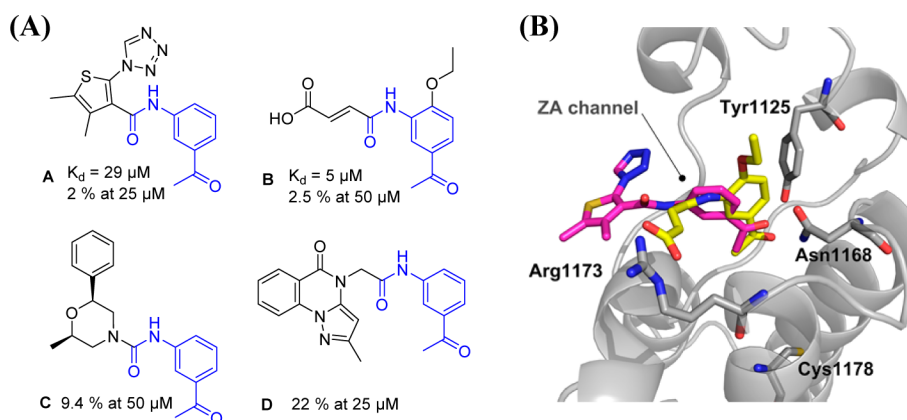
We decided to take a different approach based on high-throughput docking on the target<sup>22,23</sup> and started our CREBBP ligand-identification campaign by fragment-based docking into the structure of the CREBBP bromodomain. Herein we present the result of a computer-aided, structure-based approach which has enabled the discovery of several nanomolar ligands of the CREBBP bromodomain upon optimization of binding by modulation of the electrostatic interaction with Arg1173 (numbering from PDB structures 3SVH and 3P1C), a residue located at the entrance of the binding site that is considered to be key for attaining selectivity toward CREBBP.<sup>20,21,24–26</sup>

## ■ RESULTS AND DISCUSSION

**Computation.** Details about the docking campaign carried out to identify the initial bromodomain ligand hits can be found in ref 27. Initially, 17 compounds (cluster representatives) were chosen for in vitro validation. The acetyl benzene **A** showed activity and was selected for further investigations based on its amenability to subsequent chemical editing. Three additional acetylbenzene derivatives (compounds **B**, **C**, and **D**) were also

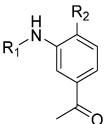
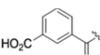
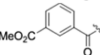
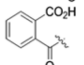
**Special Issue:** Epigenetics

**Received:** January 29, 2015



**Figure 1.** (A) Commercially available compound **A** identified in the high-throughput docking campaign and its available analogues **B–D**. Equilibrium dissociation constant ( $K_d$ ) values and/or single-dose data (where lower percentages indicate stronger hits)<sup>30</sup> were determined in the competition binding assay (BROMOscan at DiscoverX<sup>28,29</sup>). The common structural features of **A–D** are shown in blue. (B) Docked poses of **A** (carbon atoms in magenta) and **B** (carbon atoms in yellow) into the CREBBP bromodomain (gray). The side chains of the conserved Tyr1125 and Asn1168 residues together with Arg1173 and Cys1178 are shown as sticks. The ZA channel, a region of the binding site that has proven to be important for bromodomain ligand design, is also indicated.<sup>3,12,16</sup>

**Table 1.** First Approach toward the Optimization of Compound **B**

						
Cmpd	R <sub>1</sub>	R <sub>2</sub>	$\Delta T_m$ (°C) <sup>[a]</sup>	$K_d$ (μM) <sup>[b]</sup>	IC <sub>50</sub> (μM) <sup>[c]</sup>	
<b>B</b>	Fumaric acid	OEt	1.8 ± 0.2	4.7	5.2	–
<b>1</b>	Fumaric acid	OMe	1.1 ± 0.1	–	–	60
<b>2</b>	Fumaric acid	Me	0.2 ± 0.1	–	–	>100
<b>3</b>	Fumaric acid	F	−0.1 ± 0.1	–	–	>100
<b>4</b>	Fumaric acid	H	0.1 ± 0.1	–	–	30
<b>5</b>	1,2-Cyclopropanedicarboxylic acid	OEt	1.1 ± 0.1	–	–	>100
<b>6</b>		OEt	3.8 ± 0.1	0.88	0.67	8.7
<b>7</b>		OEt	2.8 ± 0.5 <sup>[d]</sup>	0.69	0.49	5.0
<b>8</b>		OEt	1.9 ± 0.1	–	–	64

<sup>a</sup>Median value of the shift in the melting temperature (number of measurements, >10) for the CREBBP bromodomain. SEM values are given. <sup>b</sup> $K_d$  values were determined by a competition binding assay<sup>28,29</sup> in duplicate. Both recorded values are given in the table. <sup>c</sup>IC<sub>50</sub> values were determined at BPS Bioscience by means of a TR-FRET assay in duplicate. <sup>d</sup>The lower thermal shift of compound **7** in comparison to compound **6** could be due to partial hydrolysis of the methyl ester under the assay conditions.

purchased and tested (Figure 1A). The good affinity of compound **B** for CREBBP ( $K_d$  of 5 μM determined by a competition binding assay<sup>28,29</sup>) prompted us to focus our attention on the presence of the polar interactions formed between the molecule's carboxylic acid and the Arg1173 residue, which could be playing an important role in binding (Figure 1B). The acrylamide moiety in compound **B** could potentially establish a covalent bond with nucleophilic amino acid residues of the bromodomain, such as Cys1178. However,

the formation of this bond is very unlikely because the sulfhydryl group of Cys1178 is completely buried (Figure 1B).

**Optimization and Biophysical Characterization.** Because of its potency, ligand efficiency (0.36 kcal/mol per heavy atom), and chemically novel blueprint within the CREBBP bromodomain inhibitors' pool,<sup>31</sup> we decided to focus our optimization campaign on compound **B**. Our strategy was to preserve its acetylbenzene moiety ("head group"), since the carbonyl group is predicted to be involved in a hydrogen bond with the conserved Asn1168 in the docked pose (Figure 1B).

Several modifications were thus designed along these lines in order to generate both potent and selective CREBBP inhibitors. First, we decided to keep the fumaric acid moiety and modulate the interactions of the substituents in ortho position relative to the amide group with the hydrophobic residues located on top of the binding site, Ile1122 and Leu1120. Replacement of the ethoxy group originally present in **B** with OMe, Me, or F substituents did not have a strong effect on affinity (Table 1, compounds 1–4). We then turned our attention toward the side chain of the molecule while preserving the carboxylic acid moiety that interacts with Arg1173 according to the docked pose (Figure 1B). Remarkably, the substitution of the fumaric acid by an isophthalic group in **6** resulted in a 6-fold improvement in binding affinity representing the first nanomolar CREBBP inhibitor of our derivatization campaign. Devoid of a Michael acceptor system, **6** might be metabolically more stable preventing covalent binding to the protein through nucleophilic amino acid residues such as cysteins. We hypothesized that such improvement in affinity could be due to a more favorable interaction with the Arg1173 residue and the so-called LPF shelf together with a less unfavorable entropic penalty compared to the slightly more flexible fumaric acid derivative. The methyl isophthalate derivative **7** showed similar potency as **6**, indicating that its ester is involved in favorable polar interactions with Arg1173.

The crystal structure of compound **6** in complex with the CREBBP bromodomain (PDB code 4TQN, Figure 2) revealed

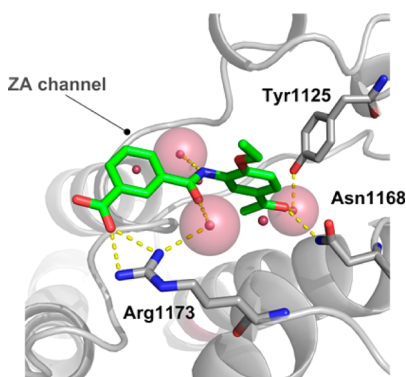


**Figure 2.** Crystal structure of CREBBP (gray) in complex with compound **6** (green) (PDB code 4TQN). The conserved Tyr1125 and Asn1168 residues together with Arg1173 are shown as sticks. The ZA channel, a region of the binding site that has proven to be important for bromodomain ligand design, is also indicated.<sup>3,12,16</sup>

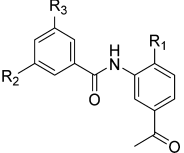
an overall binding mode similar to the docked pose of compound **6** and the fumaric acid derivative **B** obtained via flexible docking (Figure 1B).<sup>27</sup> According to the X-ray structure, compound **6** binds in the acetyllysine pocket, with its acetyl substituent involved in a hydrogen bond with the side chain of the conserved Asn1168 and a water-bridged hydrogen bond with the Tyr1125 side chain hydroxyl. The acetylbenzene head, together with its ethoxy substituent, presents high shape complementarity with the binding site. The NH group of the amide linker forms a hydrogen bond with a water molecule whose oxygen atom is located at a distance of 3.0 Å from the carbonyl oxygen of Pro1110 (in the LPF shelf): the geometry for a water-bridged hydrogen bond, however, is not ideal because the water oxygen is not in the plane of the Pro1110 carbonyl. In contrast, the carbonyl group of the amide linker is involved in a favorable water-bridged hydrogen bond with the

guanidinium of the Arg1173 side chain. Crucially, the aromaticity of the benzoic acid provides the optimal orientation for the carboxylic acid of compound **6** to form a very favorable polar interaction with the Arg1173 guanidinium of the CREBBP bromodomain. Previously, electrostatic interactions between the sulfonate group of ischemin and this arginine residue were observed.<sup>25</sup> Moreover, Conway and co-workers already reported a relatively weak ligand of CREBBP and BET bromodomains bearing a carboxylic acid that, even if not in direct contact with Arg1173, could form weak electrostatic interactions with this positively charged residue, resulting in a preferential binding toward CREBBP.<sup>26</sup>

Finite-difference Poisson calculations were performed with CHARMM<sup>32,33</sup> using the crystal structure of the CREBBP bromodomain in complex with compound **6** to evaluate the electrostatic contribution of the polar interaction to the free energy of binding of compounds **6** and **7**. The finite-difference Poisson calculation takes into account solvent screening effects which are significant because the Arg1173 side chain is partially exposed to the solvent (Figure 2). Despite the partial solvent accessibility, the electrostatic interaction between the carboxyl group of compound **6** and the guanidinium group of Arg1173 contributes  $-13.6$  kcal/mol, which is about half of the total electrostatic interaction energy ( $-26.9$  kcal/mol) between compound **6** and the CREBBP bromodomain. The finite-difference Poisson calculation was repeated on the energy minimized crystal structure. Again, the electrostatic interaction between the carboxyl group of compound **6** and the Arg1173 side chain guanidinium ( $-12.4$  kcal/mol) is about half of the total electrostatic interaction energy ( $-25.0$  kcal/mol). Analysis of the individual contributions to the binding free energy of compounds **6** and its methyl ester derivative **7** shows that the former has a slightly more favorable electrostatic contribution ( $\Delta G_{\text{electr}}^6 - \Delta G_{\text{electr}}^7 = -0.8$  kcal/mol) whereas the latter has a more favorable van der Waals contribution ( $\Delta G_{\text{vdW}}^6 - \Delta G_{\text{vdW}}^7 = 1.4$  kcal/mol) so that the difference in the calculated total binding free energy is close to zero, in line with the very similar dissociation constants of compounds **6** and **7** measured experimentally (Table 1).

With the MD simulation results<sup>27</sup> and high resolution crystal structure of the first nanomolar ligand **6** in hand we further explored the chemical space around this scaffold by introducing modifications at three different positions as illustrated in Table 2.

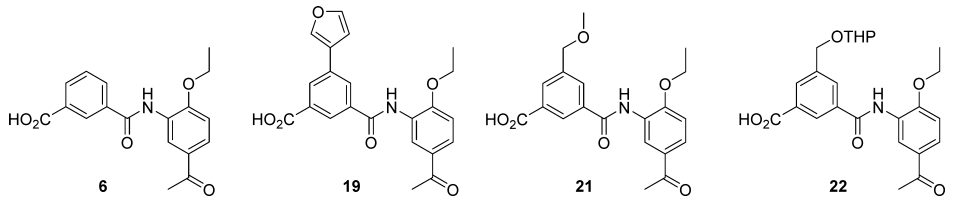
Thermal shift values similar to the one of compound **6** were observed for ligands bearing larger hydrophobic substituents in para position with respect to the acetyl group (**9–12**). More importantly, the replacement of the carboxylic acid by a tetrazole as isoster (**15**) maintained the affinity, whereas the presence of sulfonamides (**16**, **17**) resulted in a severe loss of activity. We then decided to enlarge our inhibitors toward the ZA channel by introducing both heteroaromatic (**18**, **19**) as well as linear substituents (**20–22**) bearing hydrogen bond acceptors or donors in  $R_3$  that could interact with the amino acid residues located in the ZA loop. These modifications led to the most potent inhibitors of our optimization campaign, compounds **19**, **21**, and **22**, with  $K_d$  values of 170, 540, and 400 nM, respectively (Table 3). The similar thermal shift values measured with the CREBBP bromodomain and its paralogue, EP300 (Table 2) are consistent with the fact that identical residues are present in the acetyllysine binding site of both proteins. Compounds **23** and **24** were synthesized (Figure 3) to explore the effect of the amide direction (**23**) and the

Table 2. Optimization of Compound 6<sup>a</sup>


compd	R <sub>1</sub>	R <sub>2</sub>	R <sub>3</sub>	$\Delta T_m$ (°C) <sup>b</sup>		IC <sub>50</sub> (μM) <sup>c</sup>
				CBP	EP300	
6	OEt	CO <sub>2</sub> H	H	3.8 ± 0.1	3.4 ± 0.2	8.7
9	OPr	CO <sub>2</sub> H	H	3.8 ± 0.1	3.4 ± 0.2	7.4
10	O <sup>t</sup> Bu	CO <sub>2</sub> H	H	3.5 ± 0.1	3.0 ± 0.3	NA
11	OCH <sub>2</sub> Cyc	CO <sub>2</sub> H	H	3.4 ± 0.1	3.6 ± 0.4	NA
12	OBn	CO <sub>2</sub> H	H	3.3 ± 0.1	2.6 ± 0.5	NA
13	Morph	CO <sub>2</sub> H	H	1.4 ± 0.2	1.3 ± 0.2	NA
14	Cyc	CO <sub>2</sub> H	H	3.1 ± 0.1	3.1 ± 0.2	15
15	OEt	1-tetrazole	H	3.3 ± 0.2	2.6 ± 0.4	7.5
16	OEt	PhNHSO <sub>2</sub>	H	0.0 ± 0.1	0.0 ± 0.2	>10
17	OEt	PhSO <sub>2</sub> NH	H	0.5 ± 0.1	0.4 ± 0.1	NA
18	OEt	CO <sub>2</sub> H	4-pyridyl	4.1 ± 0.1	3.9 ± 0.2	3
19	OEt	CO <sub>2</sub> H	3-furyl	5.2 ± 0.2	5.9 ± 0.2	1 <sup>d</sup>
20	OEt	CO <sub>2</sub> H	CH <sub>2</sub> OH	3.8 ± 0.1	3.7 ± 0.3	3
21	OEt	CO <sub>2</sub> H	CH <sub>2</sub> OMe	5.1 ± 0.1	4.6 ± 0.3	2 <sup>d</sup>
22	OEt	CO <sub>2</sub> H	CH <sub>2</sub> OTHP	6.0 ± 0.1	5.9 ± 0.2	1 <sup>d</sup>

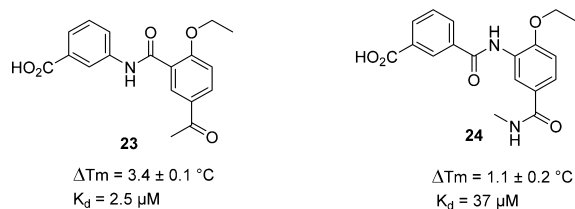
<sup>a</sup>Cyc, cyclopropyl; Morph, *N*-morpholyl; Bn, benzyl; THP, 2-tetrahydropyran. <sup>b</sup>Median value of the shift in the melting temperature (number of measurements, >4) for CBP and EP300 proteins. SEM values are indicated. <sup>c</sup>IC<sub>50</sub> values for the CREBBP bromodomain were determined by means of a TR-FRET assay in duplicate ("NA": an IC<sub>50</sub> value could not be obtained at the tested concentration range). <sup>d</sup>K<sub>d</sub> values for 19, 21, and 22 were determined by a competition binding assay<sup>28,29</sup> in duplicate with average values of 0.17, 0.54, and 0.40 μM, respectively.

Table 3. Activity and Selectivity of the Most Potent Acetylbenzene Derivatives



compd	LE <sup>a</sup>	LLE	K <sub>d</sub> (μM) ITC, CBP	K <sub>d</sub> (μM) competition binding assay <sup>b</sup>								ΔT <sub>m</sub> (°C) <sup>c</sup>			
				CBP	BRD4(1)	BRD4(2)	BRD2(1,2)	S <sup>d</sup>	CBP	EP300	BRD4(1)				
<b>6</b>	0.35	3.7	2.0	0.88	0.67	>50	>50	>50	>50	>50	>50	>65	3.8	3.4	0.4
<b>19</b>	0.32	3.2	0.3	0.17	0.17	10	9.8	>50	36	24	49	59	5.2	5.9	1.5
<b>21</b>	0.32	4.0	0.8	0.53	0.56	27	25	>50	>50	>50	>50	48	5.1	4.6	1.3
<b>22</b>	0.28	3.8		0.43	0.37								6.0	5.9	1.7

<sup>a</sup>LE = ligand efficiency, calculated as ( $\Delta G$ /number of heavy atoms), is reported in kcal/mol per heavy atom; LLE = lipophilic ligand efficiency (calculated as  $pK_d - \text{clogP}$ ).<sup>34,35</sup> clogP was calculated using ChemDraw. K<sub>d</sub> values were determined by the competition binding assay BROMOscan and were considered when calculating LE and LLE values. <sup>b</sup>K<sub>d</sub> values were determined by a competition binding assay<sup>28,29</sup> in duplicate. Both recorded values are given in the table. <sup>c</sup>Median value of the shift in the melting temperature (number of measurements, >9). SEM values did not exceed 0.3 °C. <sup>d</sup>Selectivity (S) between the CREBBP and BRD4(1) bromodomains determined by the ratio of K<sub>d</sub> values obtained via the competition binding assay.<sup>28,29</sup>



**Figure 3.** Synthesized compounds 23 and 24. The K<sub>d</sub> values determined by a competition binding assay<sup>28,29</sup> and thermal shift values for the CREBBP bromodomain are indicated.

presence of an *N*-methylcarboxamide as a surrogate of the acetyl moiety (24),<sup>31</sup> respectively. In both cases a decrease in affinity for CREBBP was observed, confirming the excellent shape complementarity between the acetylbenzene moiety and the acetyllysine binding site of the CREBBP bromodomain and its paralogue EP300.

The selectivity evaluation of compounds 1, 6, 7, 9, 14, 15, and 19–23 as determined by thermal shift measurements ( $\Delta T_m$ ) against a panel of seven bromodomains is shown in Figure 4A. Remarkable target selectivity for CREBBP and EP300 over the other five human bromodomains (each belonging to a different subfamily) was found for the



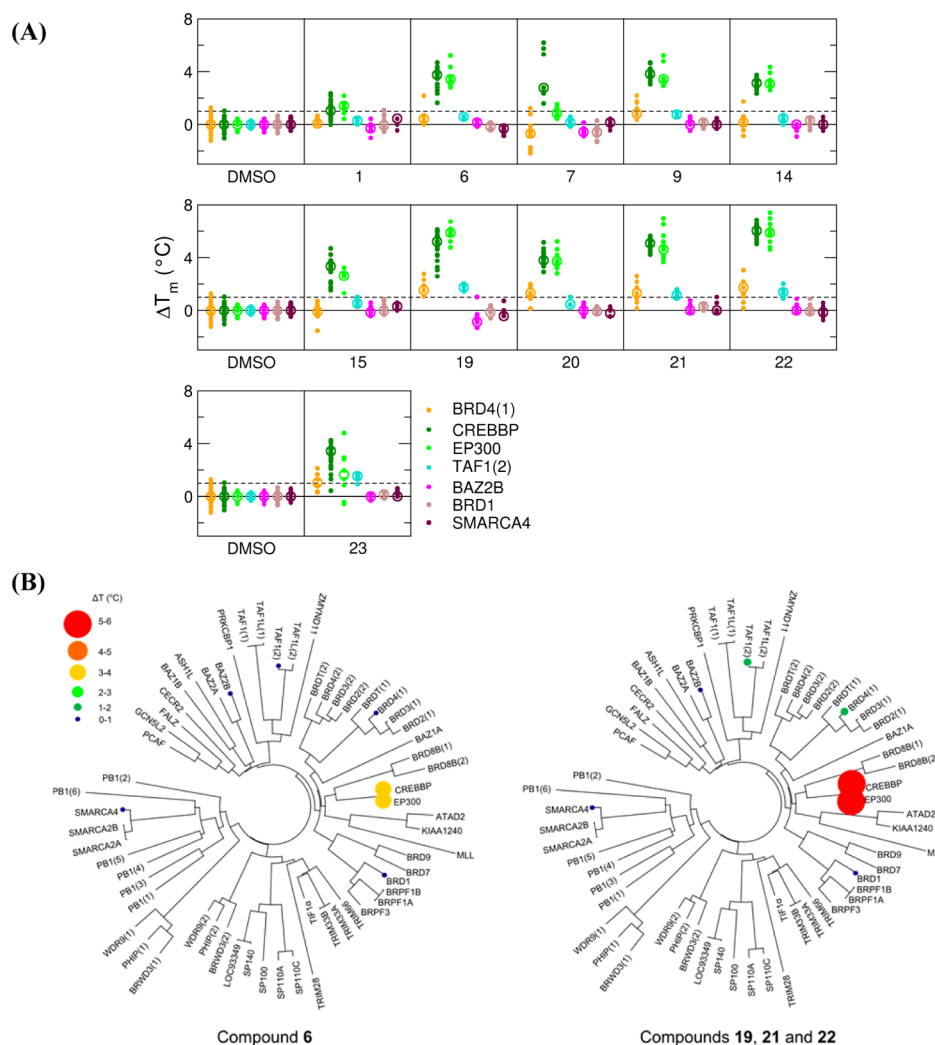


**Figure 4.** (A) Selectivity evaluation of compounds **1**, **6**, **7**, **9**, **14**, **15**, and **19–23** as determined by thermal shift measurements ( $\Delta T_m$ ) against a panel of seven bromodomains. Independent measurements are shown as dots, and the median is shown as a circle. The dashed line at 1 °C is an arbitrary threshold. (B) Bromodomain phylogenetic tree showing the selectivity evaluation of compounds **6** (left), **19**, **21**, and **22** (right) as determined by thermal shift measurements ( $\Delta T_m$ ) against a panel of different bromodomains. Sphere size and color indicate relative  $\Delta T_m$  values according to the legend, which is the same for the two figures. Compounds **19**, **21**, and **22** share the same phylogenetic tree.

nanomolar ligands **6**, **19**, **21**, and **22** according to thermal shift (Figure 4B). Interestingly, the most potent inhibitor **19**, showed only 1.7 °C thermal shift against BRD4(1), which is the most promiscuous bromodomain.<sup>20,21</sup>

The selectivity was further investigated by isothermal titration calorimetry (ITC) and a competition binding assay (Table 3).<sup>28,29</sup> Concerning ITC, the weak signal obtained for BRD4(1) does not allow a reliable fit of the titration curve (see Figure S6 in the Supporting Information).

The BRD4(1)- $K_d$ /CREBBP- $K_d$  ratio determined by competition binding yields selectivity factors of >65, 59, and 48 for compounds **6**, **19**, and **21**, respectively. Such selectivity toward the CREBBP bromodomain supports the importance of the polar interactions between the carboxylic acids and the positively charged Arg1173 for the design of selective CREBBP ligands. The leadlike properties of these molecules were determined by computing the ligand efficiency (LE)<sup>34,35</sup> and ligand-lipophilicity efficiency per unit of potency (LLE). As shown in Table 3, the high ligand efficiency (LE) was preserved throughout the optimization campaign. Moreover, the LE values (0.28–0.35 kcal/mol per heavy atom) and the ligand-

lipophilic efficiency (LLE) values (close to 4.0) of our nanomolar ligands **6**, **19**, **21**, and **22**, compare positively with those of previously disclosed ligands of the CREBBP bromodomain (see Table S5 in the Supporting Information).<sup>18,20,21</sup>

Screening of our most potent CREBBP inhibitors against a panel of 10 cancer cell lines showed lack of overall toxicity and significant growth inhibition for the leukemia cell lines MOLM-13, ML2, and HL-60 specifically for compounds **6**, **9**, **22**, and **23** (see Tables S3 and S4 in the Supporting Information). The methyl esters derived from compounds **6**, **9–11**, **19**, and **20–23** were also tested showing an equivalent or higher cell growth inhibitory activity compared to the corresponding acid counterparts, probably due to their better cell permeability. In fact, the methyl ester of **22** presented toxicity values in the low micromolar range, with  $GI_{50}$  values of 14.4 and 5.3  $\mu$ M for ML2 and MOLM-13, respectively. Even if these results are still rather preliminary, the selectivity of compound **22** toward acute myeloid leukemia suggests a potential involvement of CREBBP in this pathology (see section 10 and Tables S3 and S4 of the

Supporting Information for further details on cell based experiments).<sup>36–38</sup>

## CONCLUSIONS

In summary, we have discovered in silico and optimized by chemical synthesis a series of nanomolar potent and selective acetylbenzene ligands of the CREBBP bromodomain. Fragment-based, high-throughput docking was employed for the identification of novel scaffolds (see ref 27) whose affinity was enhanced in a straightforward manner through interactions within the ZA channel by introducing both heteroaromatic as well as linear substituents bearing hydrogen bond acceptors or donors that interact with the amino acid residues located in the ZA loop. The direct polar interaction between the benzoic acid moiety of these ligands and the Arg1173 guanidinium was exploited for the design of selective ligands of the CREBBP bromodomain. The potency, specificity, and easy synthetic availability of our compounds will be useful to unravel the role of CREBBP in several types of solid tumors and hematological malignancies.

## ASSOCIATED CONTENT

### Supporting Information

General procedures for the fragment docking, finite difference Poisson calculations, synthesis and characterization, biophysical and biological evaluation of final compounds, X-ray crystal structure refinement data, and a csv file of molecular formula strings. The Supporting Information is available free of charge on the ACS Publications website at DOI: 10.1021/acs.jmedchem.5b00172.

### Accession Codes

PDB code for CREBBP in complex with the ligand 6 is 4TQN.

## AUTHOR INFORMATION

### Corresponding Authors

\*A.C.: e-mail, caflisch@bioc.uzh.ch; phone, +41 44 635 55 21.

\*C.N.: e-mail, cristina.nevado@chem.uzh.ch; phone, +41 44 635 39 45.

### Notes

The authors declare no competing financial interest.

## ACKNOWLEDGMENTS

Lisa Gartenmann and Jean-Rémy Marchand are acknowledged for carrying out the thermal shift measurements and finite-difference Poisson calculations, respectively. We thank Lisa Caflisch and Dr. Ilian Jelezarov for support for protein purification and calorimetry, respectively. This work was supported by the Swiss Cancer Society (Krebsliga) and the Swiss National Science Foundation. D.S. is a recipient of the SystemsX.ch translational postdoc fellowship. We thank the Structural Genomics Consortium at Oxford University for providing the plasmids of all the bromodomains but EP300 (provided by AddGene).

## ABBREVIATIONS USED

ALTA, anchor-based library tailoring approach; BET, bromodomain and extra terminal domain; Bn, benzyl; BRD2(1)/(2), first/second bromodomain of BRD2; BRD4(1)/(2), first/second bromodomain of BRD4; CHARMM, chemistry at Harvard molecular mechanics; CREBBP/CBP, CREB binding protein; Cyc, cyclopropyl; DMSO, dimethyl sulfoxide; EP300, E1A binding protein p300; <sup>i</sup>Bu, isobutyl; ITC, isothermal

titration calorimetry; Morph, *N*-morpholyl; Pr, propyl; SEED, solvation energy for exhaustive docking; SEM, standard error of the mean; THP, 2-tetrahydropyrane

## REFERENCES

- (1) Holliday, R. The Inheritance of Epigenetic Defects. *Science* **1987**, *238*, 163–170.
- (2) Kouzarides, T. Chromatin modifications and their function. *Cell* **2007**, *128*, 693–705.
- (3) Filippakopoulos, P.; Knapp, S. Targeting bromodomains: epigenetic readers of lysine acetylation. *Nat. Rev. Drug Discovery* **2014**, *13*, 337–356.
- (4) Vidler, L. R.; Brown, N.; Knapp, S.; Hoelder, S. Druggability Analysis and Structural Classification of Bromodomain Acetyl-lysine Binding Sites. *J. Med. Chem.* **2012**, *55*, 7346–7359.
- (5) Prinjha, R. K.; Witherington, J.; Lee, K. Place your BETs: the therapeutic potential of bromodomains. *Trends Pharmacol. Sci.* **2012**, *33*, 146–153.
- (6) Müller, S.; Filippakopoulos, P.; Knapp, S. Bromodomains as therapeutic targets. *Expert Rev. Mol. Med.* **2011**, *13*, e29.
- (7) Furdas, S. D.; Carlino, L.; Sippl, W.; Jung, M. Inhibition of bromodomain-mediated protein-protein interactions as a novel therapeutic strategy. *MedChemComm* **2012**, *3*, 123–134.
- (8) Conway, S. J. Bromodomains: Are Readers Right for Epigenetic Therapy? *ACS Med. Chem. Lett.* **2012**, *3*, 691–694.
- (9) Arrowsmith, C. H.; Bountra, C.; Fish, P. V.; Lee, K.; Schapira, M. Epigenetic protein families: a new frontier for drug discovery. *Nat. Rev. Drug Discovery* **2012**, *11*, 384–400.
- (10) Zhang, G. T.; Sanchez, R.; Zhou, M. M. Scaling the Druggability Landscape of Human Bromodomains, a New Class of Drug Targets. *J. Med. Chem.* **2012**, *55*, 7342–7345.
- (11) Müller, S.; Knapp, S. Discovery of BET bromodomain inhibitors and their role in target validation. *MedChemComm* **2014**, *5*, 288–296.
- (12) Brand, M.; Measures, A. M.; Wilson, B. G.; Cortopassi, W. A.; Alexander, R.; Höss, M.; Hewings, D. S.; Rooney, T. P. C.; Paton, R. S.; Conway, S. J. Small Molecule Inhibitors of Bromodomain–Acetyl-lysine Interactions. *ACS Chem. Biol.* **2015**, *10*, 22–39.
- (13) Lucas, X.; Wohlwend, D.; Hugle, M.; Schmidt-kunz, K.; Gerhardt, S.; Schule, R.; Jung, M.; Einsle, O.; Gunther, S. 4-Acyl Pyrroles: Mimicking Acetylated Lysines in Histone Code Reading. *Angew. Chem., Int. Ed.* **2013**, *52*, 14055–14059.
- (14) Mirguet, O.; Gosmini, R.; Toum, J.; Clement, C. A.; Barnathan, M.; Brusq, J. M.; Mordaunt, J. E.; Grimes, R. M.; Crowe, M.; Pineau, O.; Ajakane, M.; Daugan, A.; Jeffrey, P.; Cutler, L.; Haynes, A. C.; Smithers, N. N.; Chung, C. W.; Bamborough, P.; Uings, I. J.; Lewis, A.; Witherington, J.; Parr, N.; Prinjha, R. K.; Nicodeme, E. Discovery of Epigenetic Regulator I-BET762: Lead Optimization to Afford a Clinical Candidate Inhibitor of the BET Bromodomains. *J. Med. Chem.* **2013**, *56*, 7501–7515.
- (15) Zhao, Y. J.; Yang, C. Y.; Wang, S. M. The Making of I-BET762, a BET Bromodomain Inhibitor Now in Clinical Development. *J. Med. Chem.* **2013**, *56*, 7498–7500.
- (16) Hewings, D. S.; Rooney, T. P. C.; Jennings, L. E.; Hay, D. A.; Schofield, C. J.; Brennan, P. E.; Knapp, S.; Conway, S. J. Progress in the Development and Application of Small Molecule Inhibitors of Bromodomain–Acetyl-lysine Interactions. *J. Med. Chem.* **2012**, *55*, 9393–9413.
- (17) Gerona-Navarro, G.; Yoel-Rodriguez, Mujtaba, S.; Frasca, A.; Patel, J.; Zeng, L.; Plotnikov, A. N.; Osman, R.; Zhou, M. M. Rational Design of Cyclic Peptide Modulators of the Transcriptional Coactivator CBP: A New Class of p53 Inhibitors. *J. Am. Chem. Soc.* **2011**, *133*, 2040–2043.
- (18) Fedorov, O.; Lingard, H.; Wells, C.; Monteiro, O. P.; Picaud, S.; Keates, T.; Yapp, C.; Philpott, M.; Martin, S. J.; Felletar, I.; Marsden, B. D.; Filippakopoulos, P.; Müller, S.; Knapp, S.; Brennan, P. E. [1,2,4]Triazolo[4,3-a]phthalazines: Inhibitors of Diverse Bromodomains. *J. Med. Chem.* **2014**, *57*, 462–476.

- (19) Hewings, D. S.; Fedorov, O.; Filippakopoulos, P.; Martin, S.; Picaud, S.; Tumber, A.; Wells, C.; Olcina, M. M.; Freeman, K.; Gill, A.; Ritchie, A. J.; Sheppard, D. W.; Russell, A. J.; Hammond, E. M.; Knapp, S.; Brennan, P. E.; Conway, S. J. Optimization of 3,5-Dimethylisoxazole Derivatives as Potent Bromodomain Ligands. *J. Med. Chem.* **2013**, *56*, 3217–3227.
- (20) Rooney, T. P. C.; Filippakopoulos, P.; Fedorov, O.; Picaud, S.; Cortopassi, W. A.; Hay, D. A.; Martin, S.; Tumber, A.; Rogers, C. M.; Philpott, M.; Wang, M. H.; Thompson, A. L.; Heightman, T. D.; Pryde, D. C.; Cook, A.; Paton, R. S.; Müller, S.; Knapp, S.; Brennan, P. E.; Conway, S. J. A Series of Potent CREBBP Bromodomain Ligands Reveals an Induced-Fit Pocket Stabilized by a Cation- $\pi$  Interaction. *Angew. Chem., Int. Ed.* **2014**, *53*, 6126–6130.
- (21) Hay, D. A.; Fedorov, O.; Martin, S.; Singleton, D. C.; Tallant, C.; Wells, C.; Picaud, S.; Philpott, M.; Monteiro, O. P.; Rogers, C. M.; Conway, S. J.; Rooney, T. P. C.; Tumber, A.; Yapp, C.; Filippakopoulos, P.; Bunnage, M. E.; Müller, S.; Knapp, S.; Schofield, C. J.; Brennan, P. E. Discovery and Optimization of Small-Molecule Ligands for the CBP/p300 Bromodomains. *J. Am. Chem. Soc.* **2014**, *136*, 9308–9319.
- (22) Zhao, H. T.; Gartenmann, L.; Dong, J.; Spiliotopoulos, D.; Caflisch, A. Discovery of BRD4 bromodomain inhibitors by fragment-based high-throughput docking. *Bioorg. Med. Chem. Lett.* **2014**, *24*, 2493–2496.
- (23) Spiliotopoulos, D.; Caflisch, A. Molecular Dynamics Simulations of Bromodomains Reveal Binding-Site Flexibility and Multiple Binding Modes of the Natural Ligand Acetyl-Lysine. *Isr. J. Chem.* **2014**, *54*, 1084–1092.
- (24) Sachchidanand; Resnick-Silverman, L.; Yan, S.; Mutjaba, S.; Liu, W. J.; Zeng, L.; Manfredi, J. J.; Zhou, M. M. Target structure-based discovery of small molecules that block human p53 and CREB binding protein association. *Chem. Biol.* **2006**, *13*, 81–90.
- (25) Borah, J. C.; Mujtaba, S.; Karakikes, I.; Zeng, L.; Müller, M.; Patel, J.; Moshkina, N.; Morohashi, K.; Zhang, W. J.; Gerona-Navarro, G.; Hajjar, R. J.; Zhou, M. M. A Small Molecule Binding to the Coactivator CREB-Binding Protein Blocks Apoptosis in Cardiomyocytes. *Chem. Biol.* **2011**, *18*, 531–541.
- (26) Hewings, D. S.; Wang, M. H.; Philpott, M.; Fedorov, O.; Uttarkar, S.; Filippakopoulos, P.; Picaud, S.; Vuppusetty, C.; Marsden, B.; Knapp, S.; Conway, S. J.; Heightman, T. D. 3,5-Dimethylisoxazoles Act As Acetyl-lysine-mimetic Bromodomain Ligands. *J. Med. Chem.* **2011**, *54*, 6761–6770.
- (27) Xu, M.; Unzue, A.; Dong, J.; Spiliotopoulos, D.; Nevado, C.; Caflisch, A. Discovery of CREBBP bromodomain inhibitors by high-throughput docking and hit optimization guided by molecular dynamics. *J. Med. Chem.* **2015**, DOI: 10.1021/acs.jmedchem.5b00171.
- (28) Fabian, M. A.; Biggs, W. H.; Treiber, D. K.; Atteridge, C. E.; Azimioara, M. D.; Benedetti, M. G.; Carter, T. A.; Ciceri, P.; Edeen, P. T.; Floyd, M.; Ford, J. M.; Galvin, M.; Gerlach, J. L.; Grotzfeld, R. M.; Herrgard, S.; Insko, D. E.; Insko, M. A.; Lai, A. G.; Lelias, J. M.; Mehta, S. A.; Milanov, Z. V.; Velasco, A. M.; Wodicka, L. M.; Patel, H. K.; Zarrinkar, P. P.; Lockhart, D. J. A small molecule-kinase interaction map for clinical kinase inhibitors. *Nat. Biotechnol.* **2005**, *23*, 329–336.
- (29) Quinn, E.; Wodicka, L.; Ciceri, P.; Pallares, G.; Pickle, E.; Torrey, A.; Floyd, M.; Hunt, J.; Treiber, D. Abstract 4238: BROMOScan - a high throughput, quantitative ligand binding platform identifies best-in-class bromodomain inhibitors from a screen of mature compounds targeting other protein classes. *Cancer Res.* **2013**, *73*, 4238.
- (30) See Supporting Information for further details.
- (31) Ferguson, F. M.; Fedorov, O.; Chaikuad, A.; Philpott, M.; Muniz, J. R. C.; Felletar, I.; von Delft, F.; Heightman, T.; Knapp, S.; Abell, C.; Ciulli, A. Targeting Low-Druggability Bromodomains: Fragment Based Screening and Inhibitor Design against the BAZ2B Bromodomain. *J. Med. Chem.* **2013**, *56*, 10183–10187.
- (32) Brooks, B. R.; Brooks, C. L.; Mackerell, A. D.; Nilsson, L.; Petrella, R. J.; Roux, B.; Won, Y.; Archontis, G.; Bartels, C.; Boresch, S.; Caflisch, A.; Caves, L.; Cui, Q.; Dinner, A. R.; Feig, M.; Fischer, S.; Gao, J.; Hodoscek, M.; Im, W.; Kuczera, K.; Lazaridis, T.; Ma, J.; Ovchinnikov, V.; Paci, E.; Pastor, R. W.; Post, C. B.; Pu, J. Z.; Schaefer, M.; Tidor, B.; Venable, R. M.; Woodcock, H. L.; Wu, X.; Yang, W.; York, D. M.; Karplus, M. CHARMM: The Biomolecular Simulation Program. *J. Comput. Chem.* **2009**, *30*, 1545–1614.
- (33) Im, W.; Beglov, D.; Roux, B. Continuum Solvation Model: computation of electrostatic forces from numerical solutions to the Poisson-Boltzmann equation. *Comput. Phys. Commun.* **1998**, *111*, 59–75.
- (34) Hopkins, A. L.; Groom, C. R.; Alex, A. Ligand efficiency: a useful metric for lead selection. *Drug Discovery Today* **2004**, *9*, 430–431.
- (35) Leeson, P. D.; Springthorpe, B. The influence of drug-like concepts on decision-making in medicinal chemistry. *Nat. Rev. Drug Discovery* **2007**, *6*, 881–890.
- (36) Borrow, J.; Stanton, V. P.; Andresen, J. M.; Becher, R.; Behm, F. G.; Chaganti, R. S. K.; Civin, C. I.; Distech, C.; Dube, I.; Frischauf, A. M.; Horsman, D.; Mitelman, F.; Volinia, S.; Watmore, A. E.; Housman, D. E. The translocation t(8;16)(p11, p13) of acute myeloid leukaemia fuses a putative acetyltransferase to the CREB binding protein. *Nat. Genet.* **1996**, *14*, 33–41.
- (37) Sobulo, O. M.; Borrow, J.; Tomek, R.; Reshmi, S.; Harden, A.; Schlegelberger, B.; Housman, D.; Doggett, N. A.; Rowley, J. D.; ZeleznikLe, N. J. MLL is fused to CBP, a histone acetyltransferase, in therapy-related acute myeloid leukemia with a t(11;16)(q23;p13.3). *Proc. Natl. Acad. Sci. U. S. A.* **1997**, *94*, 8732–8737.
- (38) Goodman, R. H.; Smolik, S. CBP/p300 in cell growth, transformation, and development. *Gene Dev.* **2000**, *14*, 1553–1577.